Remote sensing of subpixel snow cover using 0.66 and 2.1 μm channels

Yoram J. Kaufman,[1] Richard G. Kleidman,[2] Dorothy K. Hall,[1] J. Vanderlei Martins,[3] and Jonathan S. Barton[4]

Received 5 June 2001; revised 8 February 2002; accepted 17 February 2002; published 23 August 2002.

[1] Hydrologic models increasingly require knowledge of the amount of snow cover within a pixel in order to provide accurate estimates of snow covered area. Present methods for remote sensing of subpixel snow cover require knowledge of the spectral reflectance properties of the snow as well as the background material, making these methods difficult to apply globally. Similar problems were encountered in global remote sensing of aerosol particles over varying land terrain. Since both aerosol and snow are dark at 2.1 μm, we suggest a method for sub-pixel snow mapping based on experience with remote sensing of aerosols. Here the pixel reflectance at 2.1 μm is used to estimate the reflectance of the non-snow regions in the pixel at 0.66 μm. The difference between the total pixel brightness at 0.66 μm and the derived brightness of the same pixel without the snow is used to estimate the sub-pixel snow cover with an error usually < ±0.05. *INDEX TERMS:* 1610 Global Change: Atmosphere (0315, 0325); 1827 Hydrology: Glaciology (1863)

1. Introduction

[2] Remote sensing of subpixel snow cover is hindered by the unpredictable variability of the spectral properties of the subpixel non-snow surface cover. To overcome this difficulty, spectral mixing modeling techniques have been applied to the mapping of snow cover [*Rosenthal*, 1993; *Nolin et al.*, 1993]. These techniques represent the mixed pixel spectral properties and composition by combining several classes of surface covers from the image classification. The resultant fraction of snow represents the fraction of snow subpixel cover. This technique is scene based and very difficult to implement on a large scale. Automated techniques to map the subpixel snow cover are reported by *Rosenthal and Dozier* [1996], but are still problematic for use at the global scale because they apply only to a single scene or a set of scenes. In that work, a decision-tree threshold analysis approach using several spectral channels is used. The numeric thresholds were derived from the same remote sensing data sets that are used for snow detection. Though very useful for regional applications, they are not optimal for global applications because of the need to employ spectral end-members that describe the scene parameters. These end-members are unique to a scene or set of scenes, and it is very difficult to derive end-members that are globally applicable due to the extreme variability in spectral reflectance of non-snow features.

[3] We suggest that a method that must be applied globally, on a routine basis, needs to rely on a much simpler algorithm, and properties globally.

[4] Since February 2000, the Moderate Resolution Imaging Spectroradiometer (MODIS) on the Terra satellite [*Kaufman et al.*, 1998] has been acquiring data, globally at 0.25 to 1 km spatial resolution. MODIS data are used to produce operationally, binary snow maps [*Hall et al.*, in press]. Subpixel snow cover is a necessary enhancement of this product. A computationally-frugal technique for subpixel snow cover detection is required for automated, global snow cover mapping.

[5] We find the problem of remote sensing of subpixel snow to be similar to remote sensing of aerosol [*Kaufman et al.*, 1997a]. In both cases the optical properties of the background surface cover, as observed from space, are mixed with the subpixel snow or the aerosol above the surface, each with its own spectral properties. The method to separate the aerosol and surface contribution is based on the fact that fine aerosol is transparent and non-reflective at the long solar wavelengths (e.g. 2.1 μm) and therefore its contribution at 2.1 μm is negligible. Snow is also very dark in this wavelength, in particular if the snow is not fresh, with large grain sizes and therefore its contribution to the pixel reflectance is small. In the case of aerosol the reflectance of the surface under the aerosol at 0.66 μm is estimated using an empirical relationship of surface reflectance in 0.66 and 2.1 μm [*Kaufman et al.*, 1997b; *Karnieli et al.*, 2000]:

$$\rho_{0.66} = [0.5 \pm 0.05]\rho_{2.1} \quad (1)$$

This relationship provides a simple method to estimate the surface reflectance under the aerosol layer over the land. It eliminates the need to generate and update global maps of surface reflectance values. The aerosol optical thickness, a measure of the aerosol column concentration, is determined from the difference in the surface reflectance measured at the top of the atmosphere, $\rho^a_{0.66}$ that includes the surface, molecular scattering and aerosol:

$$\Delta\rho_{0.66-2.1} = \rho^a_{0.66} - 0.5\rho_{2.1} => \text{ aerosol optical thickness}$$

The technique was validated against ground based measurements around the world and resulted in accurate values of aerosol optical thickness over the land [1998; 2002]. A similar technique is developed here for the subpixel snow cover in the pixel from the difference $\Delta\rho_{0.66-2.1}$, thus avoiding the need for global maps of the surface reflectance.

2. Approach

[6] After applying an atmospheric correction to the Landsat data [e.g., *Vermote et al.*, 1997] the corrected surface reflectance, $\rho^c_{0.66}$, is derived from the measured one, $\rho^a_{0.66}$. The basic approach to derive the snow fraction from the corrected reflectance is:

$$f_{snow} = (\rho^c_{0.66} - 0.5\rho_{2.1})/\rho^{snow}_{0.66} \quad (2)$$

where $\rho_{2.1}$ is the pixel reflectance at 2.1 μm and $\rho^{snow}_{0.66}$ is the reflectance of the snow.

[7] The snow reflectance varies with the direction of observations and age of the snow. It may be determined as the average of the brightest 1–5% of the pixels in a given region with restricted

[1]NASA Goddard Space Flight Center, Greenbelt, MD, USA.
[2]Science Systems and Applications, Inc., Lanham, MD, USA.
[3]University of Maryland Baltimore County, Baltimore, MD, USA.
[4]Department of Geosciences, The Pennsylvania State University, University Park, PA, USA.

0094-8276/02/2001GL013580$05.00

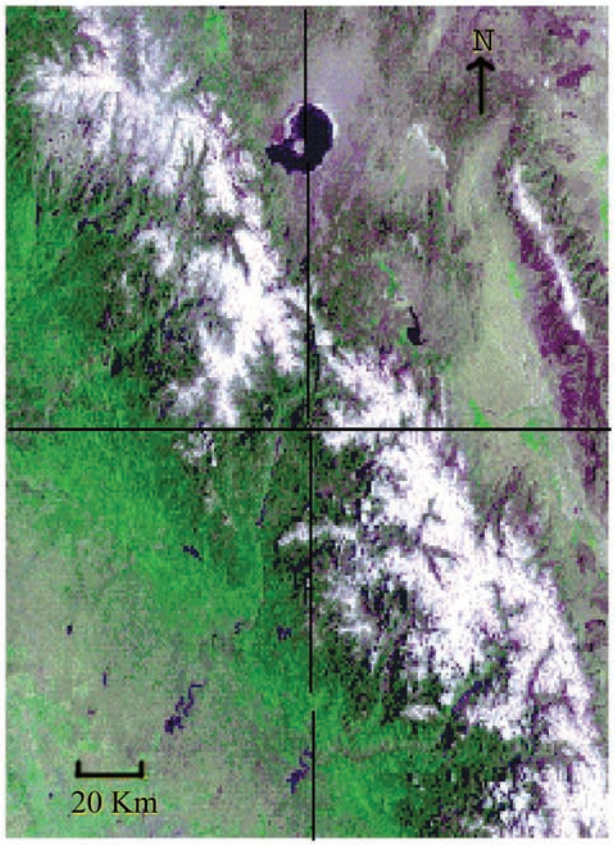

Figure 1. Color composite (red - 0.67 μm, green - 0.87 μm and blue - 0.49 μm) of the Landsat Thematic Mapper image acquired May 10, 1992. The image shows the southern Sierra Nevada range, including Mono Lake, California and the White Mountains to the east. Lines on the image show divisions into the four quadrants discussed in the analysis and in Figure 2. LL-lower left, UL-upper left, LR-lower right, UR-upper right.

view direction (e.g. ±20°), in the 250 m MODIS resolution. In the present study we found $\rho_{0.66}^{snow} = 0.6$, and estimate the error as ±0.2. Here we assume that the snow reflectance at 2.1 μm is small and does not distort the relationship between the reflectance at 2.1 μm and 0.66 μm used for the background reflectance.

[8] The applicability of the empirical relationship (1) was originally suggested to hold for $\rho_{2.1} < 0.15$. But recently we found in regions with no standing water the relationship can be extended to brighter surfaces ($\rho_{2.1} < 0.25$) [*Kaufman et al.*, 2000; *Karnieli et al.*, 2000]. This finding is also supported by recent modeling study [*Kaufman et al.*, 2002]. Original application of equation 2 to a Landsat-5 Thematic Mapper (TM) scene used by *Rosenthal and Dozier* [1996], and comparison with their validated technique, showed non-linearity in the errors in the fractional snow retrieval. We associated this non-linearity to variability of the snow reflectance, due to variability in the snow thickness, and grain size as a function of the snow fraction and due to multiple scattering between the snow and vegetation or soil. This leads to an empirical correction of the snow fraction obtained from equation 3:

$$f_{snow}^{c} = f_{snow}\rho_{0.66}^{snow} / (\rho_{0.66}^{snow} - 0.09 + 0.07 f_{snow}) \quad (3)$$

3. Application

[9] The method is applied to the same Landsat 5 TM image used by *Rosenthal and Dozier* [1996]. The image, acquired May 10, 1992, shows the southern Sierra Nevada mountain range, including Mono Lake, California (Figure 1).

[10] To reduce the atmospheric effect on the snow retrieval, we applied a simple atmospheric correction to the 0.66 μm channel, by estimating the atmospheric reflectance (for black surface) based on the top-of-atmosphere bidirectional reflectance (BRF) of the darkest water body in the image, in this case Mammoth Lake. The correction then follows *Fraser and Kaufman* [1985], assuming that for surface reflectance of 0.4 the atmospheric effect is zero. The reflectance of the water is assumed to be 0.005. The corrected reflectance at 0.66 μm, $\rho_{0.66}^{c}$ is calculated from the top of the atmosphere BRF $\rho_{0.66}^{a}$ by:

$$\rho_{0.66}^{c} = (\rho_{0.66}^{a} - \rho_{0.66}^{atm})\rho_{0.66}^{crit} / (\rho_{0.66}^{crit} - \rho_{0.66}^{atm}) \quad (4)$$

where $\rho_{0.66}^{atm}$ is the atmospheric path radiance due to aerosol and molecular scattering ($\rho_{0.66}^{atm} = 0.03$) and $\rho_{0.66}^{crit}$ is the critical surface reflectance (0.4), defined as the value of the surface reflectance for which additional aerosol does not change the apparent brightness observed from space. The subpixel snow fractions derived from equation 2 and from the correction in equation 3 are shown in Figure 2. To demonstrate the repeatability of the technique, we divided the Landsat scene into 4 equal quadrants and compared the snow fraction with the validated technique of *Rosenthal and Dozier* [1996], that is used here as the ground truth for each quadrant (called "measured snow cover"). The results show very good agreement, mainly for the empirically corrected data. The detailed errors in the 4 quadrants are plotted as a function of the measured snow cover in Figure 3. The average absolute error is between ±1% and 2% in the snow cover for the 4 quadrants. An image of the spatial distribution of the errors is seen in Figure 4. The positive and negative errors are clustered in regions with similar surface conditions that have a similar error according to the assumptions in equation 3.

4. Error Analysis

[11] There are several possible sources of errors in the present technique (equations 3–4). They are computed using equation 3:

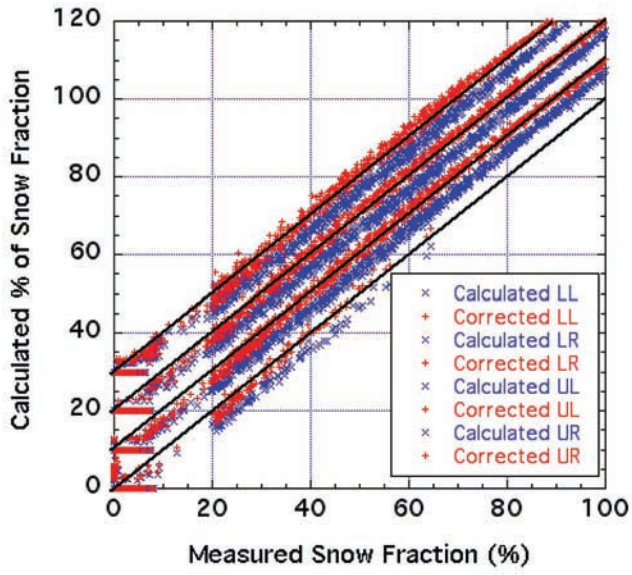

Figure 2. Scatter plot of the calculated snow cover (in %) from equation 2 (blue) and the empirically-corrected snow cover from equation 3 (red) as a function of the snow fraction derived by the validated technique of *Rosenthal and Dozier* [1996]. The results for the 4 quadrants were shifted by 10% on the abscissa, for better viewing of the scatter plots. Therefore all the black lines start in their corresponding zero point.

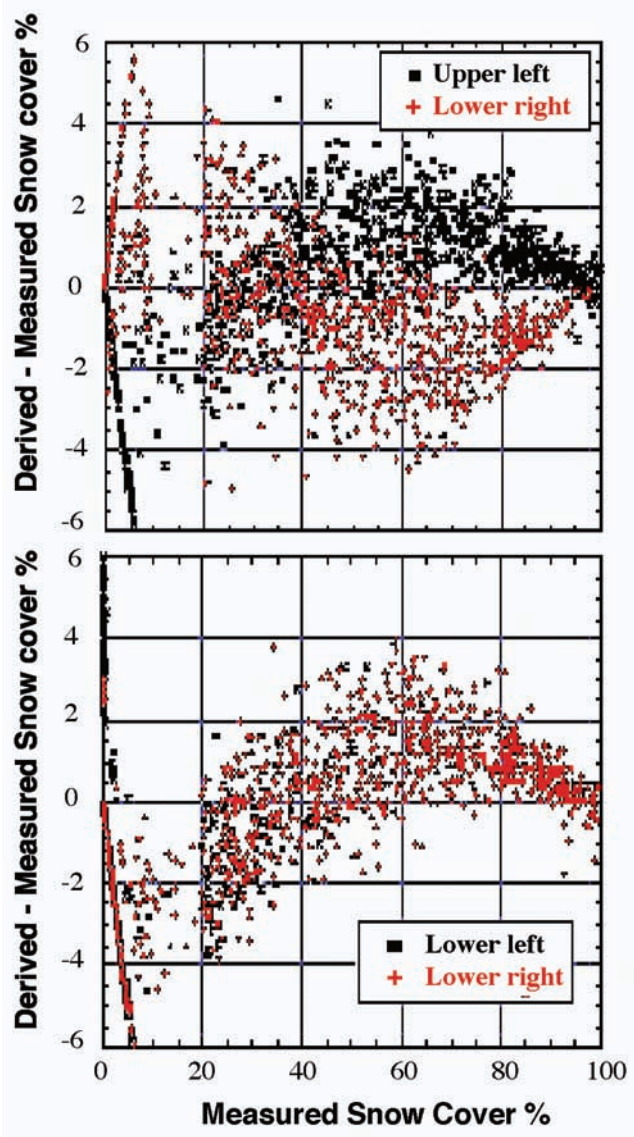

Figure 3. Scatter plots of the error in the derived snow cover, as a function of the measured snow cover of *Rosenthal and Dozier* [1996]. The four quadrants of the May 10, 1992 scene are shown.

- The error in the spectral ratio of 0.5 for an ensemble of points is estimated to be as ±0.05 [*Kaufman et al.*, 1997b; *Karnieli et al.*, 2000]. For snow fractions of 0.1 to 0.5, this corresponds to an error of $\Delta f^{c}_{snow} = \pm 0.01$.
- Error in the image estimate of the snow reflectance of $\Delta\rho^{snow}_{0.66} = \pm 0.2$. For snow fraction of 0.1 to 0.3 it corresponds to an error of $\Delta f^{c}_{snow} = \pm 0.02$ to $\Delta f^{c}_{snow} = \pm 0.09$ respectively.
- Error in the snow reflectance at 2.1 μm of $\Delta\rho^{snow}_{2.1} = \pm 0.1$ for snow fractions of 0.1 to 0.3 corresponds to an error of $\Delta f^{c}_{snow} = \pm 0.01$ to $\Delta f^{c}_{snow} = \pm 0.03$.
- Equation 4 generates a correction of 0.01 to 0.03 for snow fractions of 0.1 to 0.3. Problems with its global applicability will result in errors that are estimated to be half as large.
- Uncertainty in the atmospheric correction algorithm due to error in the estimated aerosol optical thickness of ±0.1 is $\Delta\rho^{snow}_{2.1} = \pm 0.015$.

Therefore, the root mean square total error for an ensemble of pixels is expected to be $\Delta f^{c}_{snow} = \pm 0.03$ for snow fractions of 0.1, to $\Delta f^{c}_{snow} = \pm 0.1$ for snow fraction of 0.3. The errors in the application shown in Figure 3 are within the range of this error estimate.

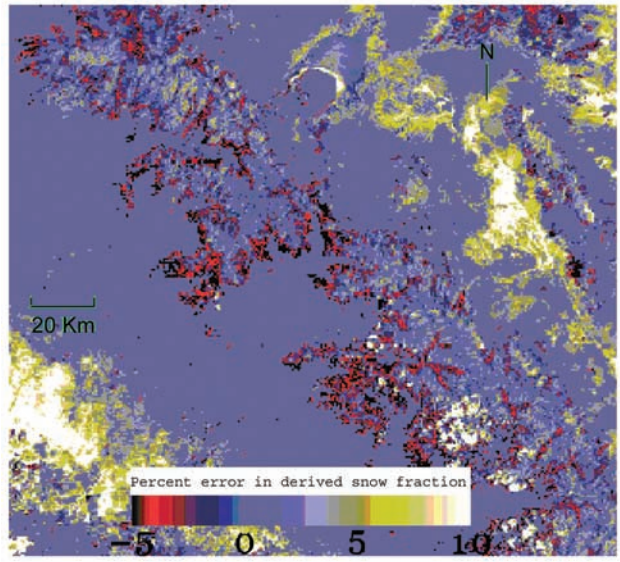

Figure 4. Color composite showing the distribution of snow understimate (dark blue to red and black) and overestimate (Yellow to white).

5. Consistency Check

[12] A robust subpixel snow detection algorithm should perform with similar accuracies in different image spatial resolutions. In Figure 5 we compare two applications of the algorithm: (1) The algorithm was applied to the original image with a resolution of 30 m to derive the snow fraction, then the resolution of the product was reduced to 500 m resolution by averaging 17 × 17 pixels. (2) In the second application, the image resolution was reduced, by averaging the spectral radiance to 500 m and the snow detection

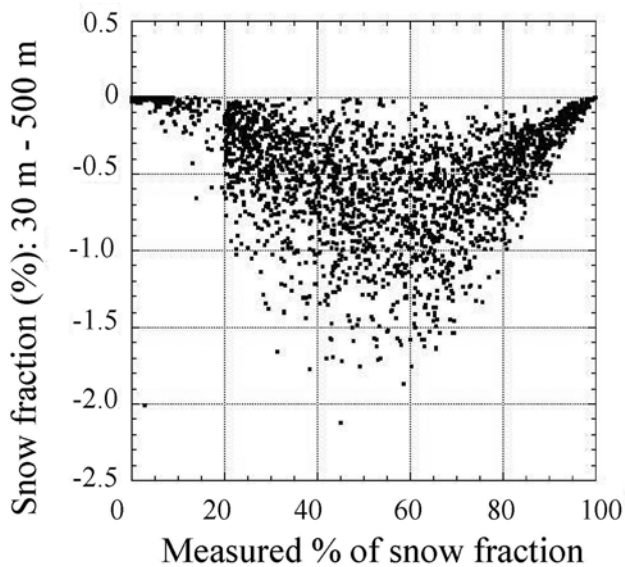

Figure 5. The difference between snow fraction (in %) derived from the 30 m resolution data and the 500 m resolution data. For the 30 m resolution data the snow fraction was retrieved and then averaged for the 500 m pixels.

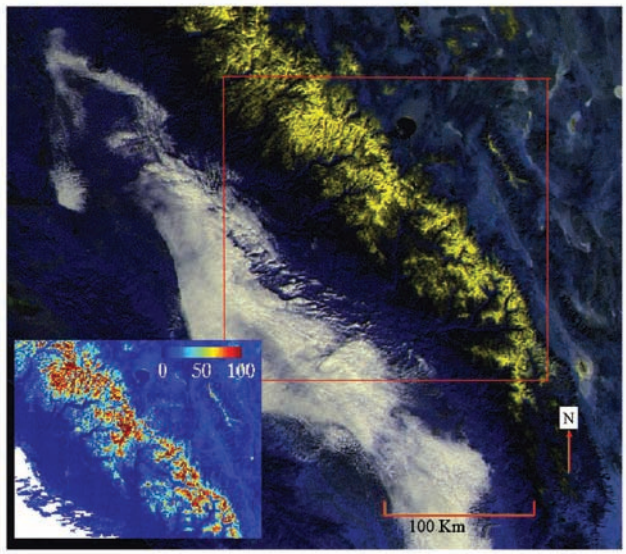

Figure 6. MODIS 0.5 km resolution image of the same area as in Figure 1 in California, for December 16, 2000. The color composite used in the main image is: red - 0.55 μm green - 0.66 μm and blue - 1.6 μm. By using the 1.6 μm channel, snow (yellow) is easily distinguished from coastal and valley clouds and fog (white). Inset image is a subset of this area corresponsing to the red box, showing percent snow derived from the MODIS image using the present algorithm. This area overlaps the TM image used to develop the algorithm (Figures 1 and 4).

algorithm was then applied. Figure 5 shows the difference between these two applications as a function of the measured snow fraction at the 500 m resolution. As expected for complete snow cover there is no effect of the different resolutions. However even for intermediate snow fractions the errors do not exceed 1 or 2 percent. Therefore the algorithm is robust across this one order of magnitude change in the spatial scales. The robustness is the result of reliance on the spectral properties.

6. Conclusions

[13] A new technique to measure sub-pixel snow cover is presented. It is based on principles of remote sensing of aerosol over the land. Both aerosol and sub-pixel snow are dark at 2.1 μm and much brighter at 0.66 μm. A relationship between directional reflectance of the non-snow (vegetation and soils) part of the surface, at 0.66 and at 2.1 μm is used to predict the reflectance at 0.66 μm in the absence of snow. Then the excess reflectance at 0.66 μm at the top of the atmosphere measured from the satellite sensor is attributed to snow. The successful application of this relationship to aerosol suggests that the same relationship between the non-snow surface reflectance between 2.1 and 0.66 μm can also be used for snow. The method is expected to be most accurate for snow fractions smaller than 30%. Error analysis shows that this technique can measure snow fractions of 0.1 with an error of ±0.03 while that of 0.3 with an error of ±0.1. Validation using the 4 quadrants of a single Landsat TM image reveal errors of 2–4%. The algorithm was shown to be independent of the spatial scale of the data, at least in the case being studied, and equally accurate for detecting sub-pixel snow in resolutions of 30 m and 500 m. Global validation is yet to be made, however an application to MODIS data collected in the same location of the Landsat data of Figure 1 is shown in Figure 6. MODIS is providing 500-m resolution snow-cover products on a daily basis using a binary snow-detection algorithm. The addition of a subpixel snow-cover algorithm is a planned enhancement, and several algorithms are being tested [*Barton et al.*, 2001]. In Figure 6 we show the subpixel fraction of snow derived from the MODIS data.

[14] **Acknowledgments.** We would like to George Riggs of SSAI for useful suggestions concerning this work.

References

Barton, J. S., D. K. Hall, and G. A. Riggs, Remote Sensing of Fractional Snow Cover using Moderate Resolution Imaging Spectroradiometer (MODIS) Data, *Proc. of the 57th Eastern Snow Conference*, May 17–19, 2000, Syracuse, NY, 2001.

Chu, A., Y. J. Kaufman, L. A. Remer, and B. N. Holben, Remote sensing of smoke from MODIS Airborne Simulator During SCAR-B Experiment, *J. Geophys. Res.*, *103*, 31,979–31,988, 1998.

Chu, D. A., Y. J. Kaufman, C. Ichoku, L. A. Remer, D. Tanre, and B. N. Holben, Validation of MODIS aerosol optical depth retrieval over land, *GRL*, in press, 2002.

Fraser, R. S., and Y. J. Kaufman, The Relative Importance of Aerosol Scattering and Absorption in Remote Sensing, *IEEE J. Geosc. Rem. Sens.*, *GE-23*, 525–633, 1985.

Hall, D. K., G. A. Riggs, V. V. Salomonson, N. E. Digirolamo, and K. J. Bayr, MODIS Snow-Cover Poducts. *J. Rem. Sens of the Environ.*, in press.

Karnieli, A., Y. J. Kaufman, L. A. Remer, and A. Wald, Aerosol Free Vegetation Index (AFRI), submitted to *J. Rem. Sens of the Environ.*, June 2000.

Kaufman, Y. J., N. Gobron, B. Pinty, J.-L. Widlowski, and M. M. Verstraete, Theoretical basis for the surface spectral reflectance relationships used in the MODIS aerosol algorithm, submited to *GRL*, 2002.

Kaufman, Y. J., D. D. Herring, K. J. Ranson, and G. J. Collatz, Earth Observing System AM mission to Earth, *IEEE IGARS special issue on EOS*, *36*, 1045–1055, 1998.

Kaufman, Y. J., A. Karnieli, and D. Tanré, Detection of dust over the desert by EOS-MODIS, *IEEE TGARS*, *38*, 525–531, 2000.

Kaufman, Y. J., D. Tanré, L. Remer, and E. Vermote, et al., Remote Sensing of Tropospheric Aerosol from EOS-MODIS over the Land, *J. Geoph. Res.*, *102*, 17,051–17,067, 1997a.

Kaufman, Y. J., A. Wald, L. A. Remer, B.-C. Gao, R.-R. Li, and L. Flynn, Remote sensing of aerosol over the continents with the 2.2 μm channel, *IEEE TGARS*, 1286–1298, 1997b.

Nolin, A. W., J. Dozier, and L. A. K. Mertes, mapping alpine snow using a spectral mixture modeling technique, *Annals of Geology*, *17*, 121–124, 1993.

Rosenthal, W., Mapping Montaine Snow Cover at Subpixel Resolution from the Landsat Thematic Mapper, M.A. Thesis, UCSB, 1993.

Rosenthal, W., and J. Dozier, Automated mapping of mountain snow cover at subpixel resolution from the Landsat Thematic mapper, *Water Resources. Res.*, *32*, 115–130, 1996.

Vermote, E. F., N. El Saleous, C. O. Justice, Y. J. Kaufman, J. L. Privette, L. Remer, J. C. Roger, and D. Tanré, Atmospheric correction of visible to mid-IR EOS-MODIS data over land surface, background, operational algorithm and validation, *JGR-Atmos.*, *102*, 17,131–17,141, 1997.

Y. J. Kaufman, NASA/GSFC code 913, Greenbelt, MD 20771, USA. (kaufman@climate.gsfc.nasa.gov)

R. G. Kleidman, Science Systems and Applications, Inc., Lanham, MD 20706, USA.

D. K. Hall, NASA/GSFC code 974, Greenbelt, MD 20771, USA.

V. J. Martins, University of Maryland Baltimore County, Baltimore, MD 21250, USA.

J. S. Barton, Department of Geosciences, The Pennsylvania State University, University Park, PA 168, USA.